JB
Journals.ASM.org

Characterization of the MSMEG_2631 Gene (*mmp*) Encoding a Multidrug and Toxic Compound Extrusion (MATE) Family Protein in *Mycobacterium smegmatis* and Exploration of Its Polyspecific Nature Using Biolog Phenotype MicroArray

Mukti Nath Mishra, Lacy Daniels

Department of Pharmaceutical Sciences, Texas A&M Health Science Center Irma Lerma Rangel College of Pharmacy, Kingsville, Texas, USA

In *Mycobacterium*, multidrug efflux pumps can be associated with intrinsic drug resistance. Comparison of putative mycobacterial transport genes revealed a single annotated open reading frame (ORF) for a multidrug and toxic compound extrusion (MATE) family efflux pump in all sequenced mycobacteria except *Mycobacterium leprae*. Since MATE efflux pumps function as multidrug efflux pumps by conferring resistance to structurally diverse antibiotics and DNA-damaging chemicals, we studied this gene (MSMEG_2631) in *M. smegmatis* mc^{2}155 and determined that it encodes a MATE efflux system that contributes to intrinsic resistance of *Mycobacterium*. We propose that the MSMEG_2631 gene be named *mmp*, for mycobacterial MATE protein. Biolog Phenotype MicroArray data indicated that *mmp* deletion increased susceptibility for phleomycin, bleomycin, capreomycin, amikacin, kanamycin, cetylpyridinium chloride, and several sulfa drugs. MSMEG_2619 (*efpA*) and MSMEG_3563 mask the effect of *mmp* deletion due to overlapping efflux capabilities. We present evidence that *mmp* is a part of an MSMEG_2626-2628-2629-2630-2631 operon regulated by a strong constitutive promoter, initiated from a single transcription start site. All together, our results show that *M. smegmatis* constitutively encodes an Na^+-dependent MATE multidrug efflux pump from *mmp* in an operon with putative genes encoding proteins for apparently unrelated functions.

Tuberculosis (TB) is still one of the biggest killers; it is estimated that *Mycobacterium tuberculosis* causes 8.8 million new cases of TB and kills 1.4 million people per year (1). Factors contributing to therapeutic complications are latency in an asymptomatic host and later reactivation to cause active disease (2, 3), intrinsic antibiotic resistance (4), and acquired drug resistance (5). Multidrug-resistant (MDR) strains further complicate therapy. Although changes responsible for acquired resistance are often understood (6–10), the basis of MDR is not yet fully defined (11, 12).

Bacteria have several antibiotic resistance strategies: (i) produce enzymes to inactivate antibiotics, (ii) alter targets to reduce antibiotic affinity, and (iii) reduce drug accumulation by decreased permeability or increased efflux (4). These strategies may be an intrinsic feature of an organism or acquired via mutations or acquisition of exogenous genes (13, 14). Low mycobacterial cell wall permeability due to its lipid-rich composition, limiting drug entry, is one reason for intrinsic resistance (15, 16), but *Mycobacterium* also has several multidrug efflux pumps (17) that enhance drug resistance by drug extrusion; however, their roles in intrinsic resistance are not well explored.

Multidrug efflux pumps extrude a wide range of structurally unrelated compounds and belong to five families: (i) ATP binding cassette (ABC), (ii) major facilitator superfamily (MFS), (iii) small multidrug resistance (SMR), (iv) resistance-nodulation-division (RND), and (v) multidrug and toxic compound extrusion (MATE). ABC family members are ATP-dependent primary transporters, but the other families are secondary transporters that use an electrochemical transmembrane gradient. MATE proteins (18) have a 12-membrane helix topology and use either H^+ or Na^+ gradients to drive efflux (19). In plants, MATE transporters secrete secondary metabolites to defend against microbial pathogens (20, 21), and in the liver and kidney they extrude xenobiotic cations (22, 23). Bacterial MATE transporters function as xenobiotic efflux pumps and can confer resistance to structurally diverse drugs, including antibiotics and DNA-damaging agents (24, 25).

MATE systems from only a few eukaryotes (26) and prokaryotes (19) have been functionally characterized. The role for most reported prokaryotic MATE transporters is not well defined, since most have been studied by heterologous expression (19). To investigate the role of a MATE transporter in *Mycobacterium* intrinsic resistance, we made an *M. smegmatis* mutant lacking this protein and characterized it using Phenotype MicroArray (PM). The present study reveals the polyspecific and Na^+-dependent nature of the *M. smegmatis* MATE transporter and transcriptional coupling of its gene with 4 upstream genes. By determining the transcription start site, we have also identified its promoter and examined its activity.

MATERIALS AND METHODS

Bacterial strains, growth conditions, plasmids, and chemicals. Table 1 describes the strains and plasmids used. Mycobacteria were cultivated at 37°C in Difco 7H9 broth supplemented with 0.2% (vol/vol) glycerol and 0.05% (wt/vol) Tween 80 or on Difco 7H10 agar plates supplemented with 0.2% (vol/vol) glycerol. *Escherichia coli* was grown at 37°C (or 30°C when using strain BW25113/pKD46) in Luria-Bertani broth. Plasmids were

Received 12 September 2012 Accepted 2 January 2013
Published ahead of print 4 January 2013
Address correspondence to Lacy Daniels, ldaniels@tamhsc.edu.

doi:10.1128/JB.01724-12

TABLE 1 Bacterial strains and plasmids used in this study

Strain or plasmids	Relevant properties	Reference or source
E. coli strains		
DH5α	Δ*lacU169 hsdR17 recA1 endA1 gyrA96 thi-1 relA1*	Lab collection
BW25113	$lacI^q$ $rrnB_{T14}$ Δ$lacZ_{WJ16}$ *hsdR514* Δ$araBAD_{AH33}$ Δ$rhaBAD_{LD78}$	27
M. smegmatis strains		
mc^2 155	Wild type	Lab collection
LD1184	mc^2 155 ΔMSMEG_2631 (or Δ*mmp*)	This work
LD1189	mc^2 155 ΔMSMEG_2619	This work
LD1192	mc^2 155 ΔMSMEG_3563	This work
LD1190	mc^2 155 ΔMSMEG_2631-ΔMSMEG_2619	This work
LD1201	mc^2 155 ΔMSMEG_2631-ΔMSMEG_3563	This work
Plasmids		
pJQ200	Suicide vector containing *sacB* and Gen^r gene	28
pKD46	λ-Red recombinase system, Amp^r, temp sensitive	27
pKD4	Plasmid containing FRT-flanked Km^r gene	27
pMN234	Plasmid for expression of *flp* gene; Km^r	29
pTB21	P_{imyc}-*gfpuv* fusion; Hyg^r; Km^r	30
pUV15	P_{smyc}-*gfpuv* fusion; Hyg^r; Km^r	30
pTL61T	*lacZ* transcriptional fusion vector with RNaseIII cleavage site; Amp^r	31
pLD132	pMN234 derivative; Gen^r	S. Jaques (unpublished data)
pLD150	pTL61T derivative; pAL5000 origin; Gen^r	S. Jaques (unpublished)
pLD182	MSMEG_2619 locus (4,035 bp) cloned in pJQ200	This work
pLD183	MSMEG_2631 locus (4,030 bp) cloned in pJQ200	This work
pLD184	MSMEG_3563 locus (4,475 bp) cloned in pJQ200	This work
pLD186	MSMEG_2619::Km^r in pLD182	This work
pLD187	MSMEG_2631::Km^r in pLD183	This work
pLD190	MSMEG_3563::Km^r in pLD184	This work
pLD216	MSMEG_2631 ORF cloned in NdeI/MluI site of pTB21	This work
pLD217	BCG_2856 (*dinF*) ORF cloned in NdeI/MluI site of pTB21	This work
pLD221	pTB21 without promoter; digested with XbaI/NheI and self-ligated	This work
pLD222	1,011-bp MSMEG_2628 upstream cloned in XbaI/NheI of pTB21	This work
pLD223	1,094-bp MSMEG_2629 upstream cloned in XbaI/NheI of pTB21	This work
pLD224	1,017-bp MSMEG_2630 upstream cloned in XbaI/NheI of pTB21	This work
pLD225	1,019-bp MSMEG_2631 upstream cloned in XbaI/NheI of pTB21	This work
pLD226	375-bp fragment encompassing TSS and promoter cloned in HindIII/XbaI site of pLD150	This work

maintained in *E. coli* DH5α with 100 μg ampicillin (Amp), 75 μg kanamycin (Km), or 25 μg gentamicin (Gen) per ml.

Bioinformatic analysis. Mycobacterial transporter families were compared using TransportDB (http://www.membranetransport.org/) (32). Protein BLAST analysis was performed via the National Center for Biotechnology Information (NCBI) (http://www.ncbi.nlm.nih.gov/BLAST). MATE homologs were retrieved from GenBank (http://www.ncbi.nlm.nih.gov/GenBank/). ClustalW2 (http://www.ebi.ac.uk/Tools/msa/clustalw2/) and MEGA (33) were used for multiple sequence alignment and phylogenetic trees. Chromosomal regions were retrieved from NCBI (http://www.ncbi.nlm.nih.gov/genome/) and J. Craig Venter Institute-Comprehensive Microbial Resource (JCVI-CMR; http://cmr.jcvi.org/tigr-scripts/CMR). Sequence Manipulation Suite (http://www.ualberta.ca/) (34) and Vector NTI Advance (Invitrogen) were used for molecular weight estimation, genomic map construction, and primer design.

Mutant construction. *M. smegmatis* mutants were constructed using homologous recombination as follows. The *mmp* (MSMEG_2631) locus was PCR amplified using 2629:F:XbaI/2633:R:BglII primers to produce a 4,030-bp fragment, which was cloned in pJQ200 (28) to generate pLD183, which was transferred to *E. coli*25113/pKD46 (to use the λ-Red recombinase system [27]) and grown at 30°C in the presence of 1 mM arabinose to make electrocompetent cells. The Km resistance gene was PCR amplified from pKD4 (27) using primers 2631:H1/2631:H2, designed to produce a 40-bp homologous region for *mmp* at both ends. PCR product was purified and electroporated into 25113/pKD46 having pLD183. Transformants were selected with Km (75 μg/ml) at 37°C on LB plates. Plasmids were isolated and examined for Km^r cassette insertion in *mmp* and designated pLD187. pLD187 was mobilized in *M. smegmatis* $mc^2$155, and transformants were selected with Km (50 μg mg^{-1}) and 2% sucrose on LB plates. Disruption was confirmed by PCR, and confirmed mutants were designated LD1158. Unmarked *mmp* deletion mutants were developed using the FLP/FLP recognition target (FLP/FRT) system. A variant of pMN234 (29) that has a Gen^r cassette (S. Jaques and L. Daniels, unpublished data) in the place of the Km^r cassette in pMN234 was mobilized in LD1158, and transformants were selected with gentamicin (20 μg ml^{-1}) on LB plates. Transformants were kept with gentamicin for 2 to 3 revivals and transferred to plain LB plates, and Km^r cassette deletion was confirmed by Km sensitivity and PCR assays. Mutants with confirmed deletion of MSMEG_2631 (ΔMSMEG2631) were designated LD1184. The same procedure was used to develop all unmarked deletion mutants.

Construction of complementation plasmids. *M. smegmatis* (*mmp*) and *Mycobacterium bovis* BCG (BCG_2856c) were PCR amplified using 2631:F:NdeI/2631:R:MluI and dinF:F:NdeI/dinF:R:MluI primers, respectively. Products digested with NdeI/MluI were ligated with digested pTB21 (intermediate mycobacterial promoter) or pUV15 (strong mycobacterial promoter) to make two expression plasmids for each open reading frame (ORF). Recombinant plasmids were purified, confirmed, and

electroporated into *M. smegmatis*. Transformants were selected with 100 μg ml^{-1} of hygromycin on LB plates.

PM tests. Phenotype MicroArray (PM; Biolog, Hayward CA) antimicrobial susceptibility tests for *M. smegmatis* were performed with modifications of earlier methods (35; S. Jaques III and L. Daniels, presented at the SCASM Conference, Austin, TX, 2008; M. Rahman, S. Jaques III, and L. Daniels, presented at the *SC-ASM Conference*, Austin, TX, 2008). Briefly, cells were streaked onto 7H10 agar plates supplemented with 0.2% (vol/vol) glycerol and grown 3 to 4 days at 37°C. Growth was removed from 7H10 plates using a cotton swab dipped in 2% Tween 80, and cells were suspended in GN/GP-IF-0a (Biolog inoculating fluid) to give 85% transmittance (Biolog turbidimeter, 20-mm diameter tube). Cell suspensions were diluted 60-fold in 120 ml of 1× IF-10b (Biolog) supplemented with 1× Biolog Redox Dye Mix H to make inoculum (100 μl/well) for 10 plates (PM-11 to -20), which measure sensitivity to antibiotics and other inhibitors. PM plates were sealed with plastic film (Axygen Inc., Union City, CA), incubated at 37°C in the OmniLog instrument (Biolog, Hayward, CA) for 168 h, and monitored for color change in the wells. Data were analyzed with OmniLog-PM software, release OL_PM_109M of 14 January 2002.

MIC determination. MICs were determined in 7H9 medium supplemented with Tween 80 and oleic acid-albumin-dextrose-catalase (OADC) with different inhibitor concentrations. Growth was monitored visually after 3 to 4 days of growth at 37°C. MIC determination was repeated five times, and only results reproduced more than three times are listed.

EtBr accumulation and efflux assay. Ethidium bromide (EtBr) accumulation and efflux assay was performed as described previously (4, 36). *M. smegmatis* was grown at 37°C in 7H9 medium to an optical density at 600 nm ($OD_{600\ nm}$) of ca. 0.7 to 0.8, and cells were harvested, washed twice with 0.1 M potassium phosphate (pH 7.2), resuspended in the same buffer at an $OD_{600\ nm}$ of 1.2, and shaken for 90 min at 37°C to starve for energy. EtBr accumulation was monitored in the presence of 50 mM NaCl, 0.2% glycerol, or NaCl plus glycerol with a NOVOstar microplate reader (BMG Labtechnologies, Inc., Durham, NC). For efflux assay, cells were loaded with EtBr by incubating cells in potassium phosphate supplemented with 5 μM ethidium bromide for 1 h at 37°C. EtBr efflux from loaded cells was monitored using the same instrument. In both assays, the final EtBr concentration was 5 μM, and excitation and emission wavelengths were 520 nm and 590 nm, respectively.

RNA extraction and RT-PCR. Total RNA was isolated from 7H9-grown, mid-exponential-phase *M. smegmatis* ($OD_{600\ nm}$, ca. 0.8 to 0.9) using the RNeasy Protect Bacteria Mini Kit (Qiagen). On-column DNase digestion was performed using RNase-Free DNase (Qiagen). Reverse transcriptase PCR (RT-PCR) was carried out with 0.3 to 0.5 μg RNA using a one-step RT-PCR kit (Qiagen). Cycling conditions were 52°C for 30 min, 95°C for 15 min, 30 cycles of 95°C for 30 s, 56 to 60°C (according to the primer) for 30 s, and 72°C for 1 min, followed by incubation at 72°C for 10 min. For two-step RT-PCR, RNA samples were reverse transcribed using the AffinityScript Multiple Temperature cDNA synthesis kit (Agilent Technologies) with template cDNA with PCR primer sets.

5′ RACE. The *mmp* transcription start site (TSS) was determined using the 3′/5′ rapid amplification of cDNA ends (3′/5′RACE) kit, 2nd Generation (Roche), according to the manufacturer's instructions. Briefly, *mmp* transcripts were reverse transcribed from total RNA into cDNA using 2631-SP1:R (Table 2). cDNA was purified using a High Pure PCR kit (Roche) and 3′-poly(dA) tailed and then used as the template in two PCRs designed to amplify the 5′ end of *mmp* and MSMEG_2628 using oligo(dT)-anchor/2631-SP2:R and oligo(dT)-anchor/2628-SP1:R primers, respectively. The oligo(dT)-anchor primer was provided in the kit to anneal to the poly(dA) tail, and 2631-SP2:R (Table 2) was complementary to a region upstream of the 2631-SP1:R binding site. First PCR products were separately used as the template in second PCRs using anchor/2631-SP3:R and anchor/2628-SP2:R primer sets. Anchor primer was provided in the kit to anneal at a region generated by oligo(dT)-anchor primer at the 3′ end of cDNA, and 2631-SP3:R and 2628-SP2:R (Table 2) were complementary to the region upstream of 2631-SP2:R and 2628-SP1:R binding sites, respectively. Product was ligated into pGEM-T Easy (Promega), and several clones were sequenced.

TABLE 2 Primers used in this study[a]

Primer	Sequence (5′ to 3′)
2629:F:XbaI	**TGCTCTAGA**CTGCACGACGCCACGCTGTACTAC
2633:R:BglII	**GGAAGATCT**CAAGTCGACGCTGCTGAAGGTGATC
2631:H1	CGCAGAACCCATCTACCTGCTTTTCGACCTCGCGATC **GTGTAGGCTGGAGCTGCTTC**
2631:H2	GCACCATGAACGTGCTGAGCCCCGACCAGATACCGAA **CATATGAATATCCTCCTTAG**
2631:F	TTGGCTGATGCGGCGGGCGACCTG
2631:R	CAAGCGCTGACCTCGTCAGGACGTG
2631:F:NdeI	**GGAATTCCATATG**TTGGCTGATGCGGCGGGCGACCTG
2631:R:MluI	**TCGACGCGT**CAAGCGCTGACCTCGTCAGGACGTG
dinF:F:NdeI	**GGAATTCCATATG**AGCCAGGTGGGGCACCGCGCG
dinF:R:MluI	**TCGACGCGT**CAACACGACGAACAGCGCATAATC
2628:F	CAGCCTGGAAGACCTGGATTC
2629:R	GTAATCCGGGTCCTCGTCGAG
2629:F	GACGCCACGCTGTACTACAC
2630:R	CACCTTTTCGTCGATGGGTTTG
2630:F	CAAACCCATCGACGAAAAGGTG
2631:R1	GATGATCAGCAGTCCGAGAC
2631-SP1:R	CCAGCACGACGTAACGCAAC
2631-SP2:R	CAGGATCGCGACACGCAACCAC
2631-SP3:R	GATGATCAGCAGTCCGAGACCGAG
2628N-sp2:R	CTGCTCTTTGAGCGTTGCTAAG
2628N-SP3:R	CTTGCTTGTGACACCGAGTTCCTTTG
Pr:F:HindIII	**CCCAAGCTT**GAAGATCGACATCATCGACTACGAC
Pr:R:XbaI	**TGCTCTAGA**GATACATGTCCGCACCGGTCCGACAG
2628us:F:XbaI	**TGCTCTAGA**GAACCGCTCATCACACTGTCGCGCAC
2628:R:NheI	**CTAGCTAGC**CACTACTTCTCCTCATCTTGAGGCGAC
2629US:F:XbaI	**TGCTCTAGA**GACACGATGTTCGTCGACATCTC
2629:R:NheI	**CTAGCTAGC**CATCAGGTACGTGCCTTCTCGAC
2630US:F:XbaI	**TGCTCTAGA**GTATCCAGGTCGACGACGAG
2630:R:NheI	**CTAGCTAGC**CATCCTCAGCGTTCGTCC
2631US:F:XbaI	**TGCTCTAGA**GATGCCGGTGACGACAACCGATC
2631:R1:NheI	**CTAGCTAGC**CAAGGGCCCGTGCGAGCGCCTGTAC

[a] Additional nucleotides not specific for *M. smegmatis* sequences are shown in bold; restriction sites are underlined.

Promoter:reporter fusion construction and promoter activity determination. A 375-bp fragment (−325 to +50 of the TSS) was amplified using Pr:F1:HindIII/Pr:R1:XbaI primers and cloned in pLD150 (a pTL61T derivative [31] of pAL5000 origin; Gen^r [Jaques and Daniels, unpublished]) to construct a promoter:*lacZ* transcriptional fusion, designated pLD226. pLD150 and pLD226 were mobilized in *M. smegmatis*. The β-galactosidase assay (37) was performed with *M. smegmatis* strains harboring pLD150 or pLD226. Cells were grown in 7H9 to mid-exponential phase and then grown for two more hours after supplementing with EtBr (2 μg ml^{-1}), norfloxacin (5 μg/ml), kanamycin (2 μg ml^{-1}), or sulfachloropyridazine (400 μg ml^{-1}). Untreated cultures were used as controls. Assay cell density was equalized by diluting with fresh medium or medium supplemented with drugs.

Upstream regions of MSMEG_2628, MSMEG_2629, and MSMEG_2630 and *mmp* (approximately 1,000 bp) were amplified using primers 2628US:F:XbaI/2628:R:NheI (1,011 bp), 2629US:F:XbaI/2629:R1:NheI (1,094 bp), 2630US:F:XbaI/2630:R1:NheI (1,017 bp), and 2631US:F:XbaI/2631:R1:NheI (1,019 bp), respectively. Amplified fragments were cloned at the XbaI/NheI site of pTB21 to construct promoter:*gfpuv* translational fusions by replacing the pTB21 promoter. Constructs with the upstream region of MSMEG_2628, MSMEG_2629, and MSMEG_2630 and *mmp* were designated pLD222, pLD223, pLD224, and pLD225, respectively. XbaI/NheI-digested pTB21 was self-ligated to construct a promoterless plasmid, designated pLD221, as a negative control; pTB21 was the positive control. GFPuv fluorescence was measured with a NOVOstar

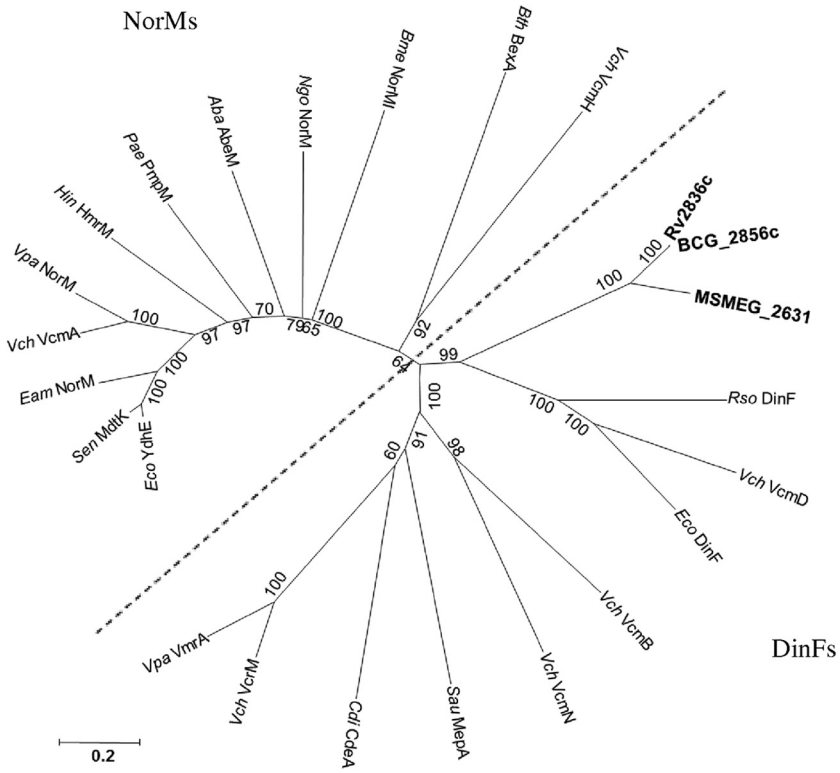

FIG 1 Phylogenetic tree based on neighbor-joining analysis of amino acid sequences of MATE transporters from *M. tuberculosis* H37Rv (Rv), *M. bovis* BCG (BCG), *M. smegmatis* (MSMEG) and studied homologs from other bacteria (*Acinetobacter baumannii* [*Aba*]; *Bacteroides thetaiotaomicron* [*Bth*]; *Brucella melitensis* [*Bme*]; *Clostridium difficile* [*Cdi*]; *Erwinia amylovora* [*Eam*]; *Escherichia coli* [*Eco*]; *Haemophilus influenzae* [*Hin*]; *Neisseria gonorrhoeae* [*Ngo*]; *Pseudomonas aeruginosa* [*Pae*]; *Ralstonia solanacearum* [*Rso*]; *Salmonella enterica* [*Sen*]; *Staphylococcus aureus* [*Sau*]; *Vibrio cholerae* [*Vch*]; *Vibrio parahaemolyticus* [*Vpa*]). Numbers show the bootstrap value for the particular branch.

microplate reader, using excitation and emission wavelengths of 395 nm and 508 nm, respectively.

RESULTS

Bioinformatic analysis of the *Mycobacterium* MATE family transporter gene. Comparison of mycobacterial genes predicted to encode transport proteins revealed a single annotated MATE efflux pump ORF in all sequenced species except *Mycobacterium leprae*: Rv2836c and MSMEG_2631 in *M. tuberculosis* H_{37}Rv and *M. smegmatis* mc^2 155, respectively. Both possess 12 likely transmembrane domains. MATE family members are divided into three clusters (NorM and DinF for prokaryotes and a Eukaryote cluster) (18). Comparison of NorM and DinF homologs to mycobacterial MATE proteins using multiple sequence alignment and a phylogenetic tree (Fig. 1) revealed that mycobacterial MATE proteins clustered with DinF proteins and made a clade with *Ralstonia solanacearum* DinF, *Escherichia coli* DinF, and *Vibrio cholerae* VcmD. Analysis of putative transmembrane regions 5 and 6 presented a slightly different picture. Mycobacterial MATEs possess a **G**W**L**G**X****P**** motif in place of GKFGXP, which is conserved only in NorMs, and also possess S**A**L**L**CPL**L**V and **G**S**A**V**A**N (conserved and similar amino acids are in bold and underlined, respectively) in place of NIXLDYXFI and GAXIAT motifs in DinF (alignments not shown). Altogether, these analyses suggest that MSMEG_2631 and Rv2836c genes encode highly similar, orthologous, MATE proteins showing overall higher similarity with known DinFs and possessing similar but less conserved motifs for both NorM and DinF groups. We propose that MSMEG_2631 gene be named *mmp*, for mycobacterial MATE protein, and refer to it by that name below.

Phenotypic characterization of MATE mutants. To examine the role of the MATE protein in intrinsic drug resistance of *M. smegmatis*, an *mmp* deletion mutant was generated in two steps: (i) an *mmp*::Km disruption mutant (LD1158) was created by homologous recombination, and (ii) the Km^r marker was removed using the FLP/FRT system to generate the Δ*mmp* mutant (LD1184). The disruption mutant (LD1158), in which 1,182 bp of *mmp* (1,368 bp) had been replaced by a Km cassette (1,477 bp), and the unmarked deletion mutant (LD1184), which has only 250 bp of *mmp*, were confirmed by PCR. To rule out antibiotic cross-reactivity due to Km resistance, only the unmarked deletion mutant (LD1184) was used to characterize its phenotype.

To identify possible *M. smegmatis* MATE efflux substrates, we used Phenotype MicroArray technology, since it facilitates phenotype analysis by testing several phenotypes and includes antibiotics, disinfectants, and other toxic compounds, on 10 PM plates with >200 different chemicals. PM tests were performed in 96-well plates containing nutrients and different inhibitors, and in which a redox indicator measures cell respiration. Potential inhibitors were provided in four concentrations, increasing from left to right on the plate; if inhibition occurs, dye development is less intense over time. Due to the lack of a standard PM protocol for *M. smegmatis* with inhibitory plates (PM-11 to -20), we attempted to optimize conditions, including cell density and inoculation

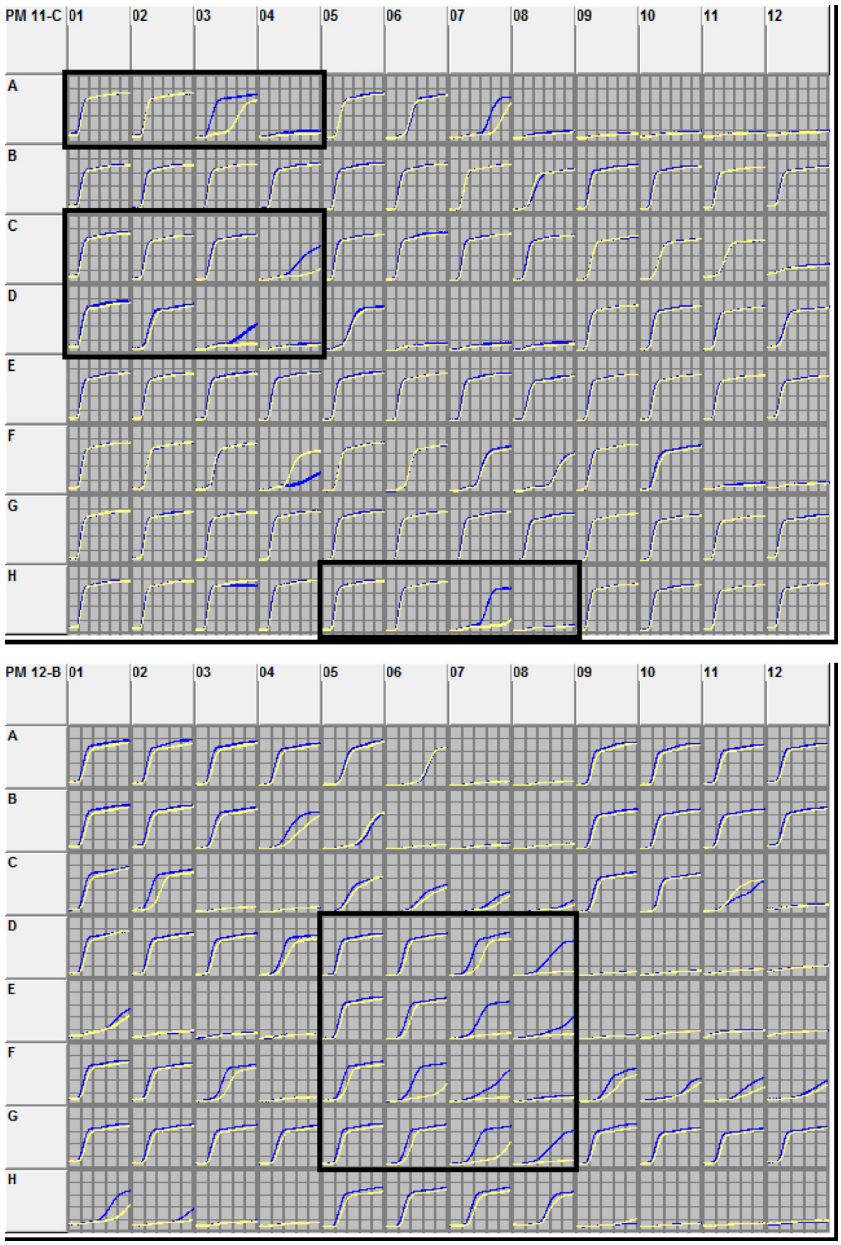

FIG 2 Phenotype MicroArray PM-11 and PM-12 data comparing the MSMEG_2631 mutant (LD1184) (yellow) with its isogenic parent (blue). Enclosed boxes indicate the wells in which differences in susceptibility were significant and consistently reproducible. (Upper panel) PM-11 has amikacin, bleomycin, capreomycin, and kanamycin in wells A1 to A4, C1 to C4, D1 to D4, and H5 to H8, respectively. (Lower panel) PM-12 has sulfamethazine, sulfadiazine, sulfathiazole, and sulfamethoxazole in wells D5 to D8, E5 to E8, F5 to F8, and G5 to G8, respectively. Antibiotic concentration in the four wells increases from left to right. Color intensity (a measure of cell metabolism) is plotted on the vertical axis versus time on the horizontal axis (168 h in this case).

fluid modifications, to provide reproducible susceptibility phenotypes. We tested PM-11 to -20 data reproducibility with replicates for wild-type cells with IF-10b or 7H9 plus 5% OADC and different cell suspension dilutions. Data with 60× dilution of 85% T cell suspension in IF-10b were fairly reproducible (data not shown). Data with 7H9 plus 5% OADC were also reproducible, but growth was slower than preferred.

M. smegmatis has more than 100 putative drug efflux genes belonging to different families. If some have overlapping substrate specificity, this may mask the effect of deleting one gene, resulting in little or no susceptibility difference. With this in mind, we created two other unmarked deletion mutants, ΔMSMEG_2619 (*efpA*) (LD1189) and ΔMSMEG_3563 (LD1192), lacking genes for reported drug efflux pumps (4), as positive controls to examine with PM plates. PM data suggested susceptibility differences for each of the three mutants in comparison to the wild type. Although differences were small in the majority of wells, suggesting enhanced mutant sensitivity, they were consistent. Drugs and chemicals identified as likely substrates by PM data for LD1189 and LD1192 include most chemicals reported earlier (4) (data not shown), which indicates PM reliability for drug susceptibility testing in *M. smegmatis*.

TABLE 3 Antimicrobial susceptibility of *M. smegmatis* mc^2 155 mutants[a]

M. smegmatis strain	Description	MIC (μg ml^{-1})								
		EtBr	NOR	CP	KM	PM	CPC	SCP	SML	SMT
mc^2 155	Wild type	4	6	8	4	0.5	10	600	700	600
LD1184	Δ2631 (MATE)	2	5	6	2	0.3	8	400	450	400
LD1189	Δ2619 (*efpA*)	2	4	5	4	0.3	7	600	700	600
LD1190	Δ2631-Δ2619	1.5	2	3	2	0.15	4	400	500	400
LD1192	Δ3563	3	6	8	2	0.5	10	450	400	450
LD1201	Δ2631-Δ3563	2	4	6	1	0.3	7	300	300	300

[a] MICs were determined by growth in 8 ml 7H9–10% OADC–0.05% Tween 80 supplemented with different concentrations of either EtBr (ethidium bromide), NOR (norfloxacin), CP (capreomycin), PM (phleomycin), CPC (cetylpyridinium chloride), SCP (sulfachloropyridazine), SML (sulfamethoxazole), or SMT (sulfamethazine). Growth was monitored by visual inspection after 3 to 4 days. Experiments were repeated at least five times to confirm the difference between wild-type and mutant strains for their susceptibility to these antimicrobial agents. Final concentration ranges (μg/ml): EtBr, 0, 0.5, 1.0, 1.5, 2.0, 2.5, 3.0, 3.5, 4.5, 5.0, 5.5, 6.0. 6.5, 7.0, 7.5, 8.0; NOR, 1, 2, 3, 4, 5, 6, 7, 8, 9, 10; CP, 1, 2, 3, 4, 5, 6, 7, 8, 9, 10; KM, 0, 0.5, 1.0, 1.5, 2.0, 2.5, 3.0, 3.5, 4.5, 5.0, 5.5, 6.0; PM, 0, 0.05, 0.1, 0.15, 0.2, 0.25, 0.30, 0.35, 0.45, 0.5, 0.55, 0.6, 0.65, 0.7, 0.75, 0.8; CPC, 0, 2, 4, 6, 8, 10, 12, 14, 16, 18, 20; all sulfa drugs (SCP, SML, and SMT), 0, 50, 100, 150, 200, 250, 300, 350, 400, 450, 500, 650, 700, 750, 800, 850, 900, 950, 1,000.

PM data for the wild type and LD1184 (Fig. 2) revealed that this mutant was more susceptible to several antibiotics and antiseptics, including capreomycin, amikacin, kanamycin, phleomycin, bleomycin, cetylpyridinium chloride, and all sulfa drugs on PM plates (sulfamethazine, sulfadiazine, sulfathiazole, sulfamethoxazole, sulfachloropyridazine, and sulfamonomethoxine). PM data revealed that (i) except for sulfa drugs, LD1189 was more susceptible to all compounds listed for LD1184 than LD1184 but not vice versa, and (ii) LD1184 and LD1192 were equally sensitive to the sulfa drugs. This observation indicated overlapping gene functions and prompted us to delete *efpA* or MSMEG_3563 in LD1184 to make double mutants LD1190 (ΔMSMEG_2631 and ΔMSMEG_2619) and LD1201 (ΔMSMEG_2631 and ΔMSMEG_3563), respectively, to examine the effect of *mmp* deletion in the presence and absence of *efpA* or MSMEG_3563. In most cases, *mmp* deletion resulted in a slight decrease in MIC values; however, double mutants showed greater MIC decreases (Table 3). MICs for LD1190 (lacking *efpA* and *mmp*) were always lower than those of LD1189 (lacking only *efpA*), indicating contributions by *mmp*. Additionally, in some cases (e.g., capreomycin) a significant MIC difference for the wild type and for LD1184 was not observed, but deletion of this gene in the *efpA*-lacking strain (LD1189) resulted in further MIC decrease. Similarly, deletion of either *mmp* or MSMEG_3563 did not produce a significant difference in some cases, but deletion of both genes resulted in a greater MIC decrease in LD1201.

Finally, ethidium bromide and norfloxacin were selected for susceptibility testing because both are NorM substrates and EtBr is a preferred DinF substrate (19). Deletion of *mmp* (mutant LD1184) rendered the strain more susceptible to EtBr (2-fold decrease in MIC) and slightly susceptible for norfloxacin (Table 2), suggesting that EtBr is a good *M. smegmatis* MATE substrate and that this protein provides low-level intrinsic resistance for structurally unrelated compounds.

Effect of *mmp* and BCG_2856c expression. Data indicating *mmp* involvement in multidrug resistance prompted us to examine complementation and the effect of its expression at higher levels. We made expression constructs with intermediate (pTB21) and strong (pUV15) promoters to express *mmp* and *M. bovis* BCG *dinF* (BCG_2856c, identical to Rv2836c). Using pUV15 resulted in growth-defective transformants, with small colonies after a week. Using pTB21 gave normal transformants, but the expression constructs grew slowly, and wild-type strains bearing either pLD216 (pTB21carrying *mmp*) or pLD217 (pTB21/BCG carrying *dinF*) were slightly more sensitive to EtBr and other drugs than strains bearing empty vector (pTB21). Complemented mutants bearing expression constructs grew slowly or were slightly more sensitive to drugs than mutants harboring empty vector. This suggests that higher expression of this gene renders cells growth defective, causing increased sensitivity.

Effect of *mmp* deletion on ethidium bromide accumulation and efflux. Several MATE members are active efflux pumps, the majority of which (NorM [38], VmrA [39], VcmA [40], VcrM [41], YdhE [36], and HmrM [42]) are Na^+ dependent. However, *Pseudomonas aeruginosa* PmpM (43) and *Acinetobacter baumannii* AbeM (44) are H^+ coupled. Thus, we examined whether *mmp* encoded an active efflux pump and if so, whether it is coupled to Na^+ or H^+. We performed EtBr accumulation and efflux assays with the wild type and LD1184 in the presence and absence of Na^+, with the anticipation that (i) *mmp* deletion would affect accumulation (positively) and efflux (negatively) if this gene encoded an efflux pump and (ii) if *mmp* encoded an Na^+-coupled MATE efflux pump, the effect of *mmp* deletion would be significant in the presence of Na^+ because other EtBr efflux pumps such as LfrA and EfpA belonging to MFS (both are H^+ coupled) would not contribute significantly without an energy source. Figure 3A shows that wild-type cells accumulate 22%, 26%, and 34% less EtBr in the presence of NaCl, glycerol, or NaCl plus glycerol, respectively, than control cells (with no NaCl or glycerol). With LD1184, glycerol reduced EtBr accumulation at a rate similar (28%) to that of the wild type (Fig. 3B). However, NaCl did not significantly affect EtBr accumulation by LD1184. EtBr efflux data from preloaded cells (Fig. 3C and D) revealed that EtBr efflux from wild-type cells was accelerated by either NaCl or glycerol but in the case of LD1184 only glycerol, and not NaCl, accelerated efflux. Additionally, efflux was maximum in the presence of NaCl plus glycerol, but only from wild-type cells. These results support the hypothesis that the *M. smegmatis* MATE efflux protein is Na^+ coupled and active.

***mmp* organization and its transcriptional linkage with upstream genes.** To investigate *mmp* inducibility by EtBr and antibiotics with promoter:reporter assays, we analyzed the 600 bp upstream to identify a putative mycobacterial promoter consensus sequence but found none. Further analysis revealed that *mmp* and three other upstream ORFs, i.e., MSMEG_2630 (encoding a DHH family protein), MSMEG_2629 (*rbfA*, encoding ribosome binding factor A), and MSMEG_2628 (*infB*, encoding translation initiation factor IF-2), were present in the same orientation. MSMEG_2629 and 2630 have an intergenic distance of 2 nucleotides, while MSMEG_2628 and 2629 and MSMEG_2630 and *mmp* overlap by 1 and 8 nucleotides, respectively. Since short intergenic distance and phylogenetically conserved gene order are important predictors of operon structure for genes in the same orientation (45), we compared the *mmp* region with that of other genomes. This gene order was fairly well conserved in more than 13 actinobacteria. Figure 4 shows that gene organization upstream of the mycobacterial MATE gene is highly conserved, but downstream

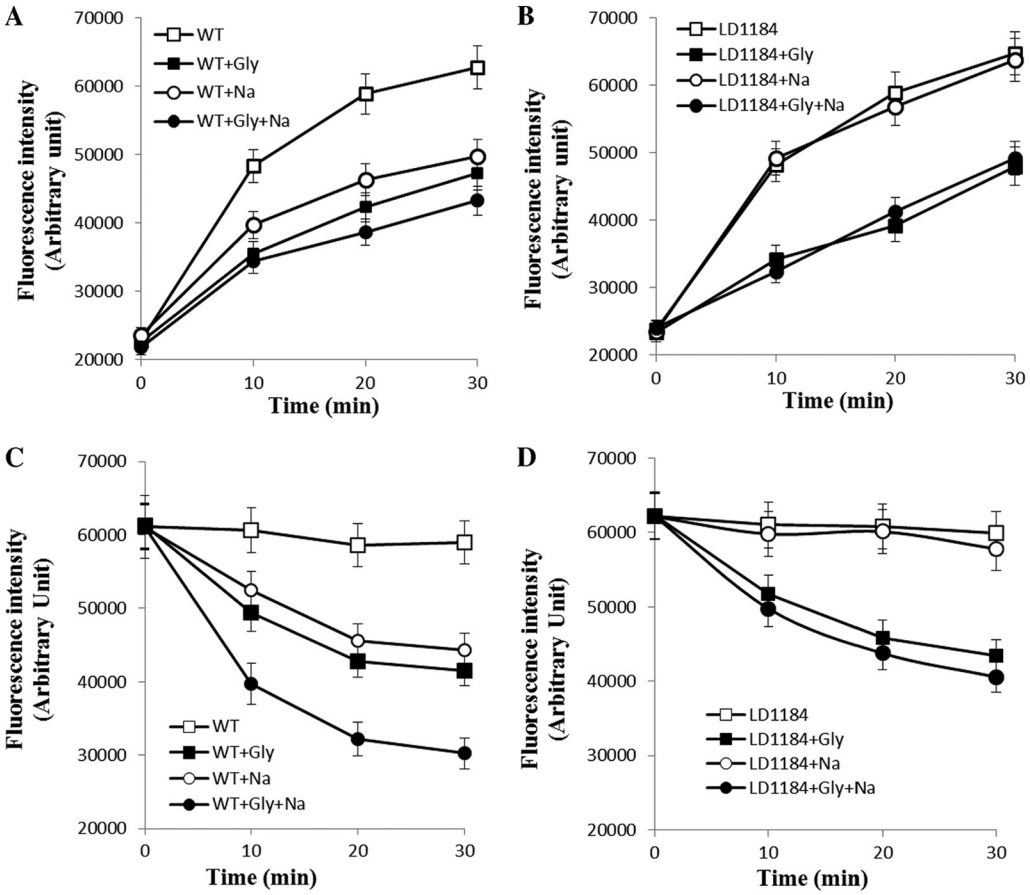

FIG 3 Effect of deletion of MSMEG_2631 gene on accumulation (A and B) and efflux (C and D) of ethidium bromide (EtBr) in the presence and absence of NaCl. Effect of 0.2% glycerol and/or 50 mM NaCl on accumulation of EtBr by the wild type (A) and LD1184 (B). Effect of 0.2% glycerol and/or 50 mM NaCl on efflux of EtBr from preloaded wild type (C) and LD1184 (D).

genes lack a conserved order. ORFs further upstream and in the same orientation have comparatively long intergenic distances. Thus, conserved synteny upstream and short intergenic distances suggest that these four adjacent codirectional genes constitute an operon and that possible functional or regulatory relationships exist among these apparently unrelated genes.

This analysis also provided insights into discrepancies about coordinates of the MSMEG_2628 locus (*infB*) in genome databases (NCBI and JCVI-CMR). Genome region comparison revealed the following: (i) while the size of *infB* in most actinobacteria varies from 2,703 to 3,015 bp, the predicted coordinates (2708747 to 2710579) for this gene in *M. smegmatis* (MSMEG_2628) represent 1,833 bp in both databases; (ii) although in the JCVI-CMR database the size for MSMEG_2628 is given as 2,805 bp, the coordinates (2708747 to 2710579) still represent 1,833 bp; (iii) in the NCBI genome database, ORF length (1,833 bp) is given according to the above coordinates; and (iv) an additional ORF (MSMEG_2627) has been annotated between MSMEG_2626 and MSMEG_2628 in the opposite transcriptional direction. On the basis of these analyses, we extended MSMEG_2628 according to the given ORF size (2,805 bp) and protein size (934 amino acids) in the JCVI-CMR database, which resulted in new coordinates (2707775 to 2710579). Additionally, we propose to remove MSMEG_2627 (not shown in figures) from the *M. smegmatis* genome because annotation of MSMEG_2627 is probably the consequence of a long intergenic gap between MSMEG_2626 and MSMEG_2628 due to erroneous short coordinates for MSMEG_2628; an MSMEG_2627 homolog was not found in any bacteria.

To examine the above prediction regarding transcriptional linkage among MSMEG_2628-2629-2630-2631, we performed one-step RT-PCR using total RNA as the template with four different primer sets to amplify fragments encompassing portions of MSMEG_2628 and 2629 (843 bp), MSMEG_2629 and 2630 (857 bp), MSMEG_2630 and *mmp* (878 bp), and *mmp* (462 bp, as internal control), covering overlapping regions. All produced fragments of expected sizes (Fig. 5A), supporting the hypothesis that these four genes are present on the same transcript. To confirm the presence of one transcript for MSMEG_2628-2629-2630-2631 and rule out possible amplification from different overlapping transcripts, we used an *mmp*-specific reverse primer (2631-SP1:R) for reverse transcription of RNA into cDNA, which was used as the template in different PCRs with above primer sets. Amplification of properly sized fragments (data not shown) confirmed the operonic organization of MSMEG_2628-2629-2630-2631.

Transcription start site identification. Although demonstration of an MSMEG_2628-2629-2630-2631 operon suggested that

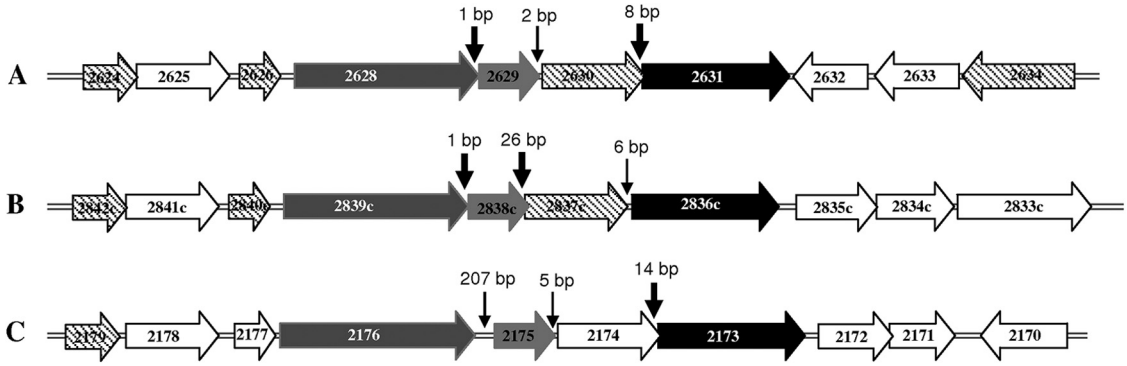

FIG 4 Genomic organization of the gene encoding the MATE family protein in *Mycobacterium smegmatis* mc^2 155 (A), *M. tuberculosis* H37Rv (B), and *Corynebacterium glutamicum* ATCC 13032 (C). Horizontal arrows represent the relative positions and orientations of annotated ORFs predicted to encode hypothetical (hatched) or known (gray, black, or white) proteins. Numbers with vertical thin and thick arrows indicate the intergenic and shared nucleotides, respectively. Black, light gray, and dark gray arrows indicate ORFs predicted for multidrug and toxic compound extrusion (MATE) family protein, ribosomal binding factor (*rbfA*), and translation initiation factor (*infB*), respectively. White arrows indicate the ORFs predicted to encode different proteins in these bacteria: MSMEG_2625/Rv2841c/Cg2178 (transcription elongation factor, NusA); MSMEG_2632 (SAM-dependent methyltransferase); MSMEG_2633 (ABC transporter ATP-binding protein); Rv2835c-Rv2834c-Rv2833c (components of an ABC transporter encoded by *ugpAEB*, respectively); Cg2177 (nucleic acid binding protein implicated in transcription termination); Cg2174 (exopolyphosphatase); Cg2172 (serine/threonine-specific protein phosphatase); Cg2171 (phosphopantetheinyl transferase); Cg2170 (tRNA pseudouridine synthase).

its transcription start site (TSS) and promoter is upstream of MSMEG_2628, it did not rule out a separate promoter for only *mmp*, upstream in MSMEG_2630. To identify the *mmp* promoter, the TSS was determined by 5′RACE using RNA from *M. smegmatis* treated with EtBr (to find an EtBr-inducible promoter, if present). Analysis of products from the second nested PCR in which anchor/2628-SP2:R or anchor/2631-SP3:R primer sets were used to amplify upstream regions of MSMEG_2628 or *mmp*, respectively, revealed a fragment produced with the former primer set, while amplification was not observed the with latter primer set. Length (>5 kb) may be a reason for lack of amplification in the case of anchor/2631-SP3:R with the same cDNA, because these primers bind to two cDNA ends (Fig. 5C) reverse transcribed from MSMEG_2628-2629-2630-2631 mRNA. Amplification with anchor/2628-SP2:R primer sets, but not anchor/2631-SP3:R with the same cDNA, indicated that TSSs and the promoter for this operon might be upstream of MSMEG_2628.

5′RACE revealed a single TSS from a G residue, in the third base of the annotated predicted start codon (GTG) of MSMEG_2626 ORF and located at position −451 bp relative to the newly predicted translational start site of MSMEG_2628 (Fig. 5B and C). Analysis of the region upstream of the identified TSS for promoter elements revealed sequences of TTCAAA at −35 and TAGACT at −10 of TSS with 18-nt spacing (Fig. 5C). Surprisingly, the presence of the TSS after the MSMEG_2626 start codon suggested that (i) MSMEG_2626 is translated from a start codon located downstream of the determined TSS and (ii) MSMEG_2626 is part of the same operon (MSMEG_2628-2627-2630-2631) predicted above to be comprised of only 4 ORFs. Initially, due to a 102-bp intergenic space between MSMEG_2626 and MSMEG_2628, we did not predict MSMEG_2626 to be in this operon, but TSS determination revealed that the operon is comprised of 5 ORFs (MSMEG_2626-2628-2629-2630-2631), starting from MSMEG_2626 and ending with *mmp*.

To identify a translational start site for MSMEG_2626, we compared its genomic organization, size, and sequences with those of homologs, revealing that (i) an MSMEG_2626 homolog is present in all sequenced actinobacteria; (ii) it is usually annotated as a conserved hypothetical protein, but in *Corynebacterium* species it is implicated in transcription termination; (iii) it showed conserved synteny (located upstream of *infB*, encoding translation initiation factor IF-2); (iv) although the *M. tuberculosis* H37Rv and *M. bovis* BCG nucleotide sequences were identical, the predicted ORF sizes in these species were 360 bp and 300 bp, respectively; (v) the annotated size of MSMEG_2626 ORF was 351 bp (starting 2 bp upstream of the TSS). A search downstream of the determined TSS in *M. smegmatis* revealed potential start codons 61 bp (GTG) or 94 bp (TTG) downstream of the TSS, making 288- or 255-bp ORFs, respectively. On the basis of this analysis, we cannot assign a start codon with certainty, but we speculate that it is GTG because the 288-bp size is close to that of BCG (300 bp).

Confirmation of promoter activity. We then investigated activity and inducibility of the identified single MSMEG_2626-2628-2629-2630-2631 promoter and whether the upstream regions of MSMEG_2629, _2630, or *mmp* had promoter activity. To examine activity and inducibility, a 375-bp fragment encompassing bp −325 to +50 from the TSS was inserted upstream of a promoterless *lacZ* reporter in pLD150 to construct a promoter:*lacZ* transcriptional reporter fusion (pLD226), and promoter activity and inducibility was monitored by measuring β-galactosidase activity of *M. smegmatis* cells harboring pLD150 or pLD226, grown in the absence or presence of different drugs. Figure 6A shows that significant activity was observed in the cells harboring pLD226. Activity was not affected by any tested drugs likely to be efflux pump substrates (data not shown). These results validate the TSS determination and indicate constitutive regulation of the MSMEG_2626-2628-2629-2630-2631 operon.

To examine whether other ORFs of this operon have promoter activity in their upstream regions, promoter:*gfpuv* translational fusions were constructed by replacing the pTB21 promoter with approximately 1,000-bp upstream regions (including the start codon) of MSMEG_2628 (pLD222), MSMEG_2629 (pLD223), MSMEG_2630 (pLD224), or *mmp* (pLD225). Promoter activity

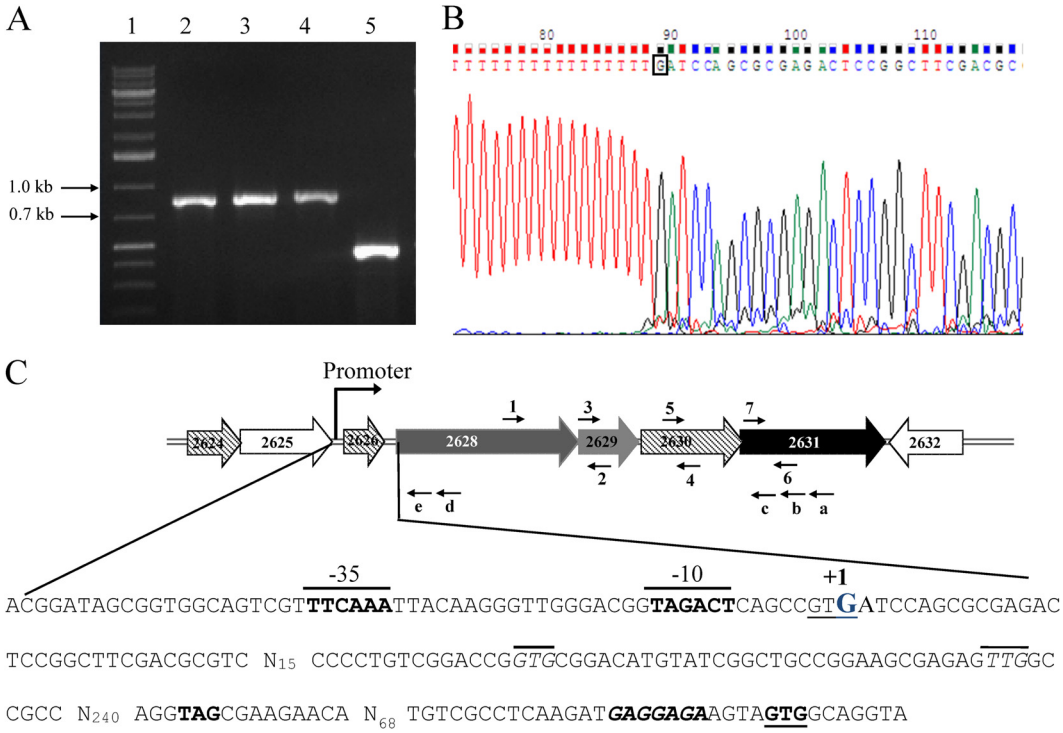

FIG 5 Demonstration of transcriptional linkage between MSMEG_2626-2628-2629-2630-2631 and determination of transcription start site (TSS) for this operon by 5′RACE. (A) Agarose gel showing reverse transcriptase PCR-amplified products obtained (numbers in parentheses refer to regions used to design primers, shown in panel C): 2628:F (1)/2629:R (2) (lane 2, 843 bp), 2629:F (3)/2630:R (4) (lane 3, 857 bp), 2630:F (5)/2631:R (6) (lane 4, 878 bp), and 2631:F (7)/2631:R (6) (lane 5, 462 bp) from RNA isolated from *Mycobacterium smegmatis* mc^2 155. Lane 1 shows the bands of 1-kb DNA ladder (GeneRuler; Fermentas). (B) Electropherogram showing TSS (enclosed in box) is representative of results from sequencing of several distinct clones obtained after 5′RACE experiment. (C) Schematic representation of MSMEG_2628-2629-2630-2631 chromosomal region of *M. smegmatis*. Large and filled arrows represent the relative size, location, and transcriptional orientation of ORFs. Small and thin arrows represent the regions used to design primers for reverse transcriptase PCR (designated by numbers) and 5′RACE experiment (designated by letters); 2631-SP1:R (a), 2631:SP2:R (b), 2631-SP3:R (c), 2628-SP1:R (d), and 2628-SP2:R (e). Nucleotides, from −509 to + 10 bp of the translational start site (bold and underlined) according to the new coordinates of MSMEG_2628, show TSS (nucleotide written in blue and indicated as +1), −35 and −10 regions (bold and overlined sequences), and a possible ribosomal binding site (bold and italicized). Start or stop codons for MSMEG_2626, according to genome databases, are indicated by underlined or bold nucleotides, respectively. Proposed start codons for MSMEG_2626 are indicated by italicized and overlined sequences.

was monitored by measuring fluorescence of cells harboring these plasmids, pLD221 (negative control), or pTB21 (positive control). From the data shown in Fig. 6B, it is obvious that only pLD222 or pTB21 expresses *gfpuv*, indicating that the sole promoter is located upstream of MSMEG_2628 and that MSMEG_2629, _2630, and *mmp* do not have a promoter in their upstream region. Quantification of GFPuv fluorescence indicated that this operon is regulated by a somewhat stronger promoter than the mycobacterial intermediate promoter in pTB21. High-level GFPuv expression by pLD222, which has the upstream region of MSMEG_2628 (1,011-bp fragment including the determined TSS and promoters) with its start codon GTG, strengthens our proposal of new MSMEG_2628 coordinates and validates the TSS and promoter for this operon.

DISCUSSION

Initially, intrinsic drug resistance was characterized as a passive mechanism associated with the absence of the drug target or lack of bacterial permeability (15, 16), but recent studies have established that it can depend on drug efflux (46–48). Efflux pumps can contribute to acquired drug resistance due to overexpression (24, 49) and to MDR (24, 50, 51). Drug efflux families, the MATE family being the most recently added group (18), have been studied for function and physiological importance (52).

For *Mycobacterium* intrinsic drug resistance, strong support exists for a major role for low cell wall permeability (15, 16) and an array of efficient multidrug efflux pumps (17). LfrA, an MFS efflux pump that confers resistance to fluoroquinolones, EtBr, acridine, and quaternary ammonium compounds, was the first such pump characterized in mycobacteria (53). More recently, other efflux pumps have been demonstrated to be involved in mycobacterial drug resistance (17). Several approaches were used in these studies: (i) monitoring drug resistance change due to efflux gene expression in a suitable host, which suggests involvement in efflux but which does not demonstrate an endogenous role or physiological importance; (ii) genome-wide expression analysis in response to drugs, which can identify inducible efflux genes and provide insights into their importance during drug exposure but which cannot identify constitutively expressed genes; (iii) monitoring drug resistance changes due to efflux gene deletion, which is a straightforward strategy but works only if the genes of interest encode a dominant efflux protein and other genes do not encode proteins with similar specificity (which may mask the effect of deletion).

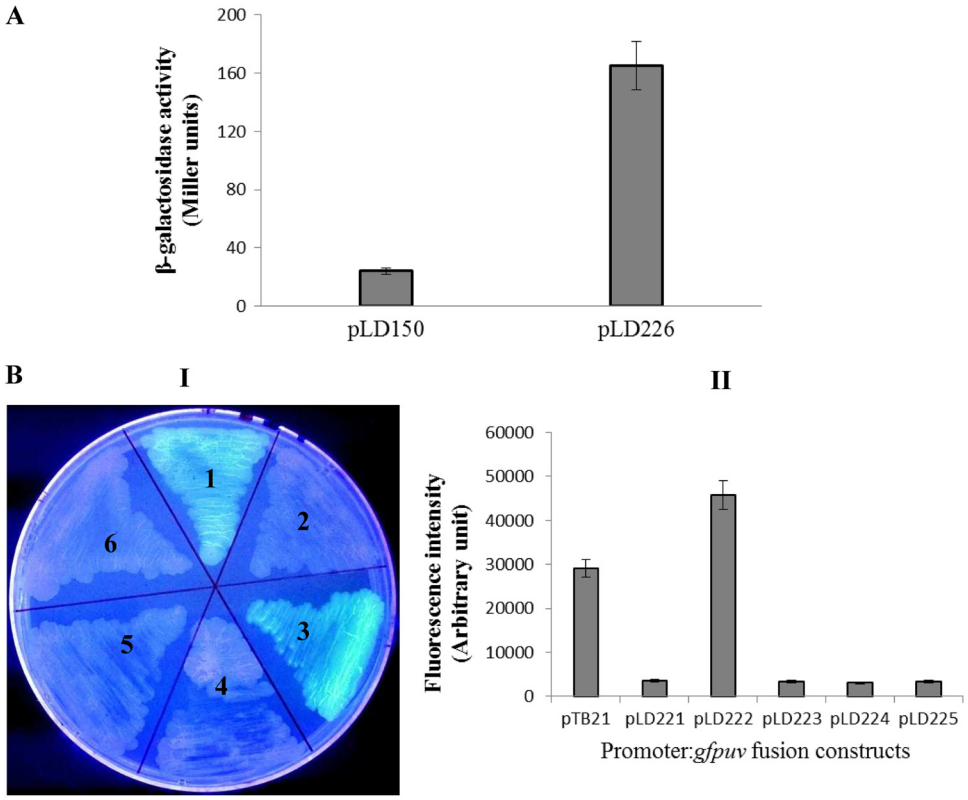

FIG 6 Estimation of promoter activity using promoter:*lacZ* transcriptional (A) and promoter:*gfpuv* translational (B) fusions. (A) β-Galactosidase activity of pLD150 (empty vector) and pLD226 (construct having a 375-bp fragment encompassing nucleotides −325 to +50 of determined TSS). (B). Expression of *gfpuv* from translational fusions constructed with upstream regions of MSMEG_2628 (pLD222), MSMEG_2629 (pLD223), MSMEG_2630 (pLD224), and MSMEG_2631 (pLD225). (I) 7H10 plate showing the expression of *gfpuv* in *M. smegmatis* harboring pTB21 (1) (positive control), pLD221 (2) (negative control, lacking the pTB21 promoter), pLD222 (3), pLD223 (4), pLD224 (5), or pLD225 (6). (II) Quantification and comparison of fluorescence intensity levels in *M. smegmatis* cells harboring translational fusions.

M. smegmatis has more than 100 predicted drug efflux pump genes from all drug efflux families, but this number is 3 times lower in *M. tuberculosis*, which might arise from niche differences or reduction in genome size. The large number of efflux pumps in *M. smegmatis* makes this bacterium a more complicated system due to overlapping specificities. Our analysis revealed a single annotated MATE family efflux gene in all *Mycobacterium* species except *M. leprae*, which suggested that although not essential, this protein is important for mycobacterial physiology.

Several MATE homologs confer resistance to fluoroquinolones (norfloxacin), cationic dyes (acriflavine and ethidium), and aminoglycosides (e.g., kanamycin and streptomycin) (19). Our data indicate that *mmp* deletion results in slightly increased susceptibility for several drugs, but its deletion in mutants lacking MSMEG_2619 (*efpA*) or MSMEG_3563 decreased MIC values further, supporting the importance of *M. smegmatis* MATE. This also suggested that in some cases deletion of only *mmp* might not result in observable MIC differences because its loss can be masked by other pumps with overlapping substrate specificity. Of importance, the use of the Biolog PM in this study helped us explore the polyspecific nature of *M. smegmatis* MATE efflux by identifying capreomycin, phleomycin, sulfa drugs, and cetylpyridinium chloride as new substrates.

Expression of *mmp* or BCG2856 (*dinF*) with an intermediate promoter (pTB21) rendered the cells slow growing and slightly more drug sensitive, which was emphasized during expression with a strong promoter (pUV15); both phenotypes likely result from excessive gene expression. Such deleterious effects have been associated with membrane disruption or undesirable metabolite export (54, 55).

All studied MATE efflux pumps, except *P. aeruginosa* PmpM and *A. baumannii* AbeM, are Na^+ coupled (19). Our EtBr accumulation and efflux data support an Na^+-dependent nature for *M. smegmatis* MATE efflux. Although the effect of *mmp* deletion on drug susceptibility was somewhat masked by MSMEG_2619 (*efpA*) and MSMEG_3563, this deletion significantly affected EtBr accumulation and efflux because of its Na^+ dependence, which enabled it to function in starved cells in the presence of NaCl, while ABC, MFS, RND, and SMR efflux pumps could not work.

The genomic organization of MATE efflux pump gene flanking regions has been studied in DinFs in several bacteria (24, 56–58). In *E. coli* and *Streptococcus pneumoniae*, *dinF* is in operons with *lexA* and *recA*, respectively (56, 57). In *Staphylococcus aureus*, the *mepRAB* operon encodes a MarR-like transcriptional regulator (*mepR*), a MATE family efflux pump (*mepA*), and a hypothetical protein (*mepB*) (24). In *Ralstonia solanacearum*, *dinF* is flanked by genes encoding a hypothetical amino acid permease and a putative transmembrane protein (58). These studies demonstrate that bacterial *dinF*-flanking regions lack conserved synteny. Our study of the *mmp* region revealed an MSMEG_2626-2628-2629-2630-

2631 operon, conserved synteny of the upstream region, and a downstream region lacking conserved gene order. Although *E. coli* (*lexA-dinF*) and *S. aureus mepRAB* present only two MATE examples, drug efflux genes in an operon with a transcriptional regulator are common in MFS. The *E. coli lexA-dinF* and *S. pneumoniae dinF-recA* operons are examples of transcriptional linkage of genes involved in DNA damage response. However, the mycobacterial MATE operon provides an exciting, new example of transcriptional coupling of a MATE efflux gene, with genes encoding proteins with apparently unrelated functions, since *infB* and *rbfA* encode translation proteins and MSMEG_2630 encodes a DHH family protein reported in *E. coli* (59) and *Thermus thermophilus* (60) to be involved in DNA base excision-repair and recycling of short oligonucleotides, respectively. Although association with a DHH gene can be explained on the basis of involvement of MATE and DHH in DNA damage response, association with *infB* and *rbfA*, which indicates involvement of MATE protein in other important cellular physiologies, cannot be explained without further research.

The *norM* promoter is induced at 18°C in *Erwinia amylovora* (61), DNA-damaging compounds induce *dinF* in *Clostridium difficile* (62) and *R. solanacearum* (58), and *mepR* negatively regulates *S. aureus mepB* MATE transcription (24). Our data indicate that MSMEG_2626-2628-2629-2630-2631 operon transcription is initiated from a single TSS and suggest that the promoter is constitutive, since no tested drugs induce promoter activity. Additionally, translational fusion data indicate that this promoter is stronger than the mycobacterial intermediate promoter in pTB21 and that the downstream ORFs in this operon lack promoters in their upstream regions. Presence of a strong promoter might explain lack of induction in response to drugs, since further induction might not be required if it is already well expressed, and lack of induction suggests that although *M. smegmatis* maintains a sufficient amount of this gene product, it does not benefit from (and may suffer from) increased expression.

This study provides evidence that *M. smegmatis* encodes an Na^+-dependent MATE family multidrug efflux pump from *mmp*, which contributes to intrinsic resistance against antibiotics, DNA-damaging chemicals, and disinfectants. *mmp* is a part of an operon that includes genes encoding proteins with apparently unrelated functions and is expressed efficiently from a strong constitutive promoter. By confirmation of transcriptional linkage, determination of the TSS, and estimation of promoter activity, we can now (i) correct the MSMEG_2628 coordinates by replacing positions 2708747 to 2710579 (given in databases) with positions 2707775 to 2710579 (proposed); (ii) remove MSMEG_2627 from the *M. smegmatis* genome, because its annotation is probably the consequence of a long intergenic gap associated with short coordinates for MSMEG_2628 and since a homolog for this protein was not found in any bacteria; (iii) indicate a new translational start site for MSMEG_2626, since the predicted start codon is located within the determined TSS.

ACKNOWLEDGMENTS

This work was supported by an NIH STTR grant shared by Barry Bochner and L.D. (GM 2R42GM073965-02A1) and by institutional support from the Rangel College of Pharmacy.

We are grateful to Sandford Jaques in our laboratory for assistance and shared reagents and plasmids and to William Jacobs, Jr., for originally providing *M. smegmatis* mc^2155.

REFERENCES

1. **WHO (World Health Organization).** 2011. WHO report 2011: global tuberculosis control. http://www.who.int/tb/publications/global_report/2011/gtbr11_full.pdf.
2. **Stewart GR, Robertson BD, Young DB.** 2003. Tuberculosis: a problem with persistence. Nat. Rev. Microbiol. **1**:97–105.
3. **Zhang Y.** 2004. Persistent and dormant tubercle bacilli and latent tuberculosis. Front. Biosci. **9**:1136–1156.
4. **Li XZ, Zhang L, Nikaido H.** 2004. Efflux pump-mediated intrinsic drug resistance in *Mycobacterium smegmatis*. Antimicrob. Agents Chemother. **48**:2415–2423.
5. **Bifani PJ, Plikaytis BB, Kapur V, Stockbauer K, Pan X, Lutfey ML, Moghazeh SL, Eisner W, Daniel TM, Kaplan MH, Crawford JT, Musser JM, Kreiswirth BN.** 1996. Origin and interstate spread of a New York City multidrug-resistant *Mycobacterium tuberculosis* clone family. JAMA **275**: 487–489.
6. **Banerjee A, Dubnau E, Quémard A, Balasubramian V, Um KS, Wilson T, Collins D, de Lisle G, Jacobs WR.** 1994. *inhA*, a gene encoding a target for isoniazid and ethionamide in *Mycobacterium tuberculosis*. Science **263**: 227–230.
7. **Dessen A, Quémard A, Blanchard JS, Jacobs WR, Jr, Sacchettini JC.** 1995. Crystal structure and function of the isoniazid target of *Mycobacterium tuberculosis*. Science **267**:1638–1641.
8. **Honore N, Cole ST.** 1994. Streptomycin resistance in mycobacteria. Antimicrob. Agents Chemother. **38**:238–242.
9. **Morris S, Bai GH, Suffys P, Portillogomez L, Fairchok M, Rouse D.** 1995. Molecular mechanisms of multiple drug resistance in clinical isolates of *Mycobacterium tuberculosis*. J. Infect. Dis. **171**:954–960.
10. **Rouse DA, Li ZM, Bai GH, Morris SL.** 1995. Characterization of the *katG* and *inhA* genes of isoniazid-resistant clinical isolates of *Mycobacterium tuberculosis*. Antimicrob. Agents Chemother. **39**:2472–2477.
11. **Pretorius GS, Van Helden PD, Sirgel FA, Eisenach KD, Victor TC.** 1995. Mutations in *katG* gene sequences in isoniazid-resistant clinical isolates of *Mycobacterium tuberculosis* are rare. Antimicrob. Agents Chemother. **39**:2276–2281.
12. **Victor TC, Pretorius GS, Felix JV, Jordaan AM, Van Helden PD, Eisenach KD.** 1996. *katG* mutations in isoniazid-resistant strains of *Mycobacterium tuberculosis* are not infrequent. Antimicrob. Agents Chemother. **40**:1572. (Letter to the editor.)
13. **Hogan D, Kolter R.** 2002. Why are bacteria refractory to antimicrobials? Curr. Opin. Microbiol. **5**:472–477.
14. **Normark BH, Normark S.** 2002. Evolution and spread of antibiotic resistance. J. Intern. Med. **252**:91–106.
15. **Brennan PJ.** 2003. Structure, function, and biogenesis of the cell wall of *Mycobacterium tuberculosis*. Tuberculosis **83**:91–97.
16. **Niederweis M.** 2003. Mycobacterial porins—new channel proteins in unique outer membranes. Mol. Microbiol. **49**:1167–1177.
17. **De Rossi E, Ainsa JA, Riccardi G.** 2006. Role of mycobacterial efflux transporters in drug resistance: an unresolved question. FEMS Microbiol. Rev. **30**:36–52.
18. **Brown MH, Paulsen IT, Skurray RA.** 1999. The multidrug efflux protein NorM is a prototype of a new family of transporters. Mol. Microbiol. **31**:394–395.
19. **Kuroda T, Tsuchiya T.** 2009. Multidrug efflux transporters in the MATE family. Biochim. Biophys. Acta **1794**:763–768.
20. **Omote H, Hiasa M, Matsumoto T, Otsuka M, Moriyama Y.** 2006. The MATE proteins as fundamental transporters of metabolic and xenobiotic organic cations. Trends Pharmacol. Sci. **27**:587–593.
21. **Morita M, Shitan N, Sawada K, Van Montagu MCE, Inzé D, Rischer H, Goossens A, Oksman-Caldentey KM, Moriyama Y, Yazaki K.** 2009. Vacuolar transport of nicotine is mediated by a multidrug and toxic compound extrusion (MATE) transporter in *Nicotiana tabacum*. Proc. Natl. Acad. Sci. U. S. A. **106**:2447–2452.
22. **Becker ML, Visser LE, van Schaik RHN, Hofman A, Uitterlinden AG, Stricker BH.** 2009. Genetic variation in the multidrug and toxin extrusion 1 transporter protein influences the glucose-lowering effect of metformin in patients with diabetes: a preliminary study. Diabetes **58**:745–749.
23. **Tsuda M, Terada T, Mizuno T, Katsura T, Shimakura J, Inui K.** 2009. Targeted disruption of the multidrug and toxin extrusion 1 (Mate 1) gene in mice reduces renal secretion of metformin. Mol. Pharmacol. **75**:1280–1286.
24. **Kaatz GW, McAleese F, Seo SM.** 2005. Multidrug resistance in *Staphy-*

lococcus aureus due to overexpression of a novel multidrug and toxin extrusion (MATE) transport protein. Antimicrob. Agents Chemother. **49**:1857–1864.
25. **McAleese F, Petersen P, Ruzin A, Dunman PM, Murphy E, Projan SJ, Bradford PA.** 2005. A novel MATE family efflux pump contributes to the reduced susceptibility of laboratory-derived *Staphylococcus aureus* mutants to tigecycline. Antimicrob. Agents Chemother. **49**:1865–1871.
26. **Moriyama Y, Hiasa M, Matsumoto T, Omote H.** 2008. Multidrug and toxic compound extrusion (MATE)-type proteins as anchor transporters for the excretion of metabolic waste products and xenobiotics. Xenobiotica **38**:1107–1118.
27. **Datsenko KA, Wanner BL.** 2000. One-step inactivation of chromosomal genes in *Escherichia coli* K-12 using PCR products. Proc. Natl. Acad. Sci. U. S. A. **97**:6640–6645.
28. **Quandt J, Hynes MF.** 1993. Versatile suicide vectors which allow direct selection for gene replacement in Gram-negative bacteria. Gene **127**:15–21.
29. **Stephan J, Stemmer V, Niederweis M.** 2004. Consecutive gene deletions in *Mycobacterium smegmatis* using the yeast FLP recombinase. Gene **343**:181–190.
30. **Kapsa I, Ehrt S, Seeber S, Schnappinger D, Martin C, Riley LW, Niederweis M.** 2001. Energy transfer between fluorescent proteins using a co-expression system in *Mycobacterium smegmatis*. Gene **278**:115–124.
31. **Linn T, Pierre RS.** 1990. Improved vector system for constructing transcriptional fusions that ensures independent translation of *lacZ*. J. Bacteriol. **172**:1077–1084.
32. **Ren Q, Chen K, and, Paulsen IT.** 2007. TransportDB: a comprehensive database resource for cytoplasmic membrane transport systems and outer membrane channels. Nucleic Acids Res. **35**:D274–D279.
33. **Tamura K, Dudley J, Nei M, Kumar S.** 2007. MEGA4: Molecular Evolutionary Genetics Analysis (MEGA) software version 4.0. Mol. Biol. Evol. **24**:1596–1599.
34. **Stothard P.** 2000. The Sequence Manipulation Suite: JavaScript programs for analyzing and formatting protein and DNA sequences. Biotechniques **28**:1102–1104.
35. **Zhou L, Lei X-H, Bochner BR, Wanner BL.** 2003. Phenotype MicroArray analysis of *Escherichia coli* K-12 mutants with deletions of all two-component systems. J. Bacteriol. **185**:4956–4972.
36. **Long F, Rouquette-Loughlin C, Shafer WM, Yu EW.** 2008. Functional cloning and characterization of the multidrug efflux pumps NorM from *Neisseria gonorrhoeae* and YdhE from *Escherichia coli*. Antimicrob. Agents Chemother. **52**:3052–3060.
37. **Miller, JH.** 1972. Experiments in molecular genetics, p 352–355. Cold Spring Harbor Laboratory, Cold Spring Harbor, NY.
38. **Morita Y, Kataoka A, Shiota S, Mizushima T, Tsuchiya T.** 2000. NorM of *Vibrio parahaemolyticus* is a Na^+-driven multidrug efflux pump. J. Bacteriol. **182**:6694–6697.
39. **Chen J, Morita Y, Huda MN, Kuroda T, Mizushima T, Tsuchiya T.** 2002. VmrA, a member of a novel class of Na^+-coupled multidrug efflux pumps from *Vibrio parahaemolyticus*. J. Bacteriol. **184**:572–576.
40. **Huda MN, Morita Y, Kuroda T, Mizushima T, Tsuchiya T.** 2001. Na^+-driven multidrug efflux pump VcmA from *Vibrio cholerae* non-O1, a non-halophilic bacterium. FEMS Microbiol. Lett. **203**:235–239.
41. **Huda MN, Chen J, Morita Y, Kuroda T, Mizushima T, Tsuchiya T.** 2003. Gene cloning and characterization of VcrM, a Na^+-coupled multidrug efflux pump, from *Vibrio cholerae* non-O1. Microbiol. Immunol. **47**:419–427.
42. **Xu XJ, Su XZ, Morita Y, Kuroda T, Mizushima T, Tsuchiya T.** 2003. Molecular cloning and characterization of the HmrM multidrug efflux pump from *Haemophilus influenza*. Microbiol. Immunol. **47**:937–943.
43. **He GX, Kuroda T, Mima T, Morita Y, Mizushima T, Tsuchiya T.** 2004. An H^+-coupled multidrug efflux pump, PmpM, a member of the MATE family of transporters, from *Pseudomonas aeruginosa*. J. Bacteriol. **186**:262–265.
44. **Su XZ, Chen J, Mizushima T, Kuroda T, Tsuchiya T.** 2005. AbeM, an H^+-coupled *Acinetobacter baumannii* multidrug efflux pump belonging to the MATE family of transporters. Antimicrob. Agents Chemother. **49**:4362–4364.
45. **Bergman NH, Passalacqua KD, Hanna PC, Qin ZS.** 2007. Operon prediction for sequenced bacterial genomes without experimental information. Appl. Environ. Microbiol. **73**:846–854.
46. **Li XZ, Livermore DM, Nikaido H.** 1994. Role of efflux pump(s) in intrinsic resistance of *Pseudomonas aeruginosa*-resistance to tetracycline, chloramphenicol, and norfloxacin. Antimicrob. Agents Chemother. **38**:1732–1741.
47. **Nikaido H.** 2001. Preventing drug access to targets: cell surface permeability barriers and active efflux in bacteria. Semin. Cell Dev. Biol. **12**:215–223.
48. **Ryan BM, Dougherty TJ, Beaulieu D, Chuang J, Dougherty BA, Barrett JF.** 2001. Efflux in bacteria: what do we really know about it? Expert Opin. Investig. Drugs **10**:1409–1422.
49. **Zgurskaya HI, Nikaido H.** 2000. Multidrug resistance mechanisms: drug efflux across two membranes. Mol. Microbiol. **37**:219–225.
50. **Li XZ, Nikaido H, Poole K.** 1995. Role of *mexA-mexB-oprM* in antibiotic efflux in *Pseudomonas aeruginosa*. Antimicrob. Agents Chemother. **39**:1948–1953.
51. **Mata MT, Baquero F, Perez-Diaz JC.** 2000. A multidrug efflux transporter in *Listeria monocytogenes*. FEMS Microbiol. Lett. **187**:185–188.
52. **Li XZ, Nikaido H.** 2009. Efflux-mediated drug resistance in bacteria: an update. Drugs **69**:1555–1623.
53. **Takiff HE, Cimino M, Musso MC, Weisbrod T, Martinez R, Delgado MB, Salazar L, Bloom BR, Jacobs WR, Jr.** 1996. Efflux pump of the proton antiporter family confers low-level fluoroquinolone resistance in *Mycobacterium smegmatis*. Proc. Natl. Acad. Sci. U. S. A. **93**:362–366.
54. **Eckert B, Beck CF.** 1989. Overproduction of transposon Tn10-encoded tetracycline resistance protein results in cell death and loss of membrane potential. J. Bacteriol. **171**:3557–3559.
55. **Hickman RK, McMurry LM, Levy SB.** 1990. Overproduction and purification of the Tn10-specified inner membrane tetracycline resistance protein Tet with fusions to β-galactosidase. Mol. Microbiol. **4**:1241–1251.
56. **Krueger JH, Elledge SJ, Walker GC.** 1983. Isolation and characterization of Tn5 insertion mutations in the *lexA* gene of *Escherichia coli*. J. Bacteriol. **153**:1368–1378.
57. **Mortier-Barriere I, De Saizieu A, Claverys JP, Martin B.** 1998. Competence-specific induction of *recA* is required for full recombination proficiency during transformation in *Streptococcus pneumoniae*. Mol. Microbiol. **27**:159–170.
58. **Brown DG, Swanson JK, Allen C.** 2007. Two host-induced *Ralstonia solanacearum* genes, *acrA* and *dinF*, encode multidrug efflux pumps and contribute to bacterial wilt virulence. Appl. Environ. Microbiol. **73**:2777–2786.
59. **Dianov G, Sedgwick B, Daly G, Olsson M, Lovett S, Lindahl T.** 1994. Release of 5′-terminal deoxyribose-phosphate residues from incised abasic sites in DNA by the *Escherichia coli* RecJ protein. Nucleic Acids Res. **22**:993–998.
60. **Wakamatsu T, Kim K, Uemura Y, Nakagawa N, Kuramitsu S, Masui R.** 2011. Role of RecJ-like protein with 5′-3′ exonuclease activity in oligo(deoxy)nucleotide degradation. J. Biol. Chem. **286**:2807–2816.
61. **Burse A, Weingart H, Ullrich MS.** 2004. NorM, an *Erwinia amylovora* multidrug efflux pump involved in in vitro competition with other epiphytic bacteria. Appl. Environ. Microbiol. **70**:693–703.
62. **Dridi L, Tankovic J, Petit JC.** 2004. CdeA of *Clostridium difficile*, a new multidrug efflux transporter of the MATE family. Microb. Drug Resist. **10**:191–196.